Benchmark Comparison of Natural Convection in a Tall Cavity

Heather E Dillon*,[1], Ashley Emery[1], and Ann Mescher[1]
[1]University of Washington
*Corresponding author: Seattle, WA 98105, hedillon@u.washington.edu

Abstract: A comparison of the commercial code COMSOL is performed with the benchmark solutions provided by the literature for a tall, differentially heated rectangular cavity for aspect ratios of 8, 15, 20, and 33. At small Rayleigh numbers the flow is dominated by conduction. As the Rayleigh number is increased the flow becomes unstable, first resulting in multicellular secondary flow patterns, and then as the Rayleigh number is further increased becoming turbulent. For this work a range of Rayleigh numbers from 1e3 to 3e5 is considered for a Prandtl number of 0.71. The predicted wavenumber, critical Rayleigh number, and characteristic streamfunctions are compared with experimental work reported in the literature. The effect of COMSOL's anisotropic and crosswind numerical diffusion values are also evaluated.

Keywords: benchmark, comsol, natural convection, tall cavity

1 Introduction

To benchmark the natural convection modeling capabilities of COMSOL, comparisons were made for free convection in tall rectangular two dimensional cavities. The geometry is a cavity of air with isothermal heated and cold walls. The differentially heated walls create a buoyancy driven convection inside the cavity. Understanding the performance of the COMSOL Multiphysics numerical diffusion for this case will allow more complex geometries, including high aspect ratio annular systems, to be modeled with greater confidence. The focus is on correctly simulating the fluid behavior for cavities with high aspect ratios (greater than 15). A summary of the computational domain for work of this type is shown in Figure 1.

The study of flow in a thermally driven cavity is a classical problem that has been explored by many researchers since the 1950s. The specific case of a square cavity has been used extensively as a numerical benchmark for computational software [6].

For natural convection studies in a cavity several parameters are used to classify the systems. The geometry of the cavity is represented by the height H, the width L and the aspect ratio (A).

$$A = \frac{H}{L} \tag{1}$$

For the computational work described in this paper the range of aspect ratios considered was $A = 8 - 33$.

Several dimensionless parameters are used to characterize the flow. The Rayleigh number (Ra) is defined below and is often used in buoyancy flows to characterize the transition between conduction dominated flow and convection dominated flow. The Prandlt number (Pr) is the ratio of the viscous diffusion and thermal diffusion. For this work, only the value of $Pr = 0.71$ (representative of air) is considered, and a range of $Ra = 1e3 - 3e5$ is explored.

$$Ra = \frac{\rho^2 g c_p \beta (\Delta T) L^3}{k\mu} \tag{2}$$

c_p is the heat capacity of the gas, g is the acceleration of gravity, β is the isobaric coefficient of thermal expansion, μ is the dynamic viscosity, k is the thermal conductivity, and ρ is the density.

$$Pr = \frac{c_p \mu}{k} \tag{3}$$

The critical Rayleigh number (Ra_c) is an important value for comparisons to experimental work. It is defined as the Rayleigh number at which the flow transitions from one stability regime to another, which corresponds to the transitions from the conduction dominated regime to convection dominated regime. In this work the critical Rayleigh number characterizes the formation of cells with oscillatory temperatures. Experimental studies often report the wavenumber (n) at Ra_c based on the wavelength (λ) of the cells.

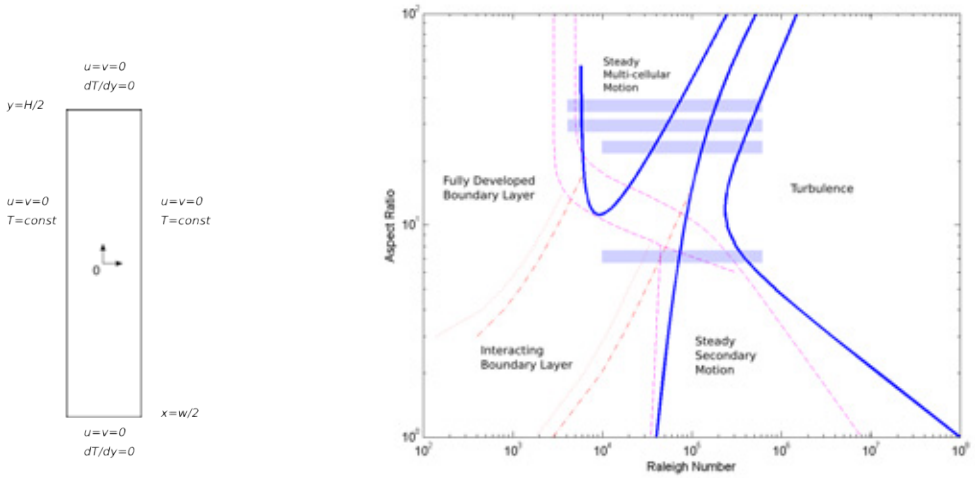

(a) (b)

Fig. 1: a) Computational domain for the tall cavity problem. b) Literature summary for the tall cavity problem. Solid and dashed lines represent stability at the Boussinesq limit (-) and higher temperature differences (- -). Dot-dash and dotted lines represent boundary layer regimes for the Boussinesq limit (-.-) and the higher temperature differences (...). The scope of the current work is shown for reference. Adapted from [4].

$$n = \frac{2\pi}{\lambda} \tag{4}$$

The heat transfer across the cavity is usually reported in terms of the Nusselt number (Nu), which is the ratio of the convective heat transfer coefficient to the conduction heat transfer coefficient.

2 Literature

The literature has shown that the stability of the flow in a cavity is governed by the Prandtl number, the Rayleigh number and the geometry of the cavity. At small Rayleigh numbers the flow is dominated by conduction. As the Rayleigh number is increased the flow becomes unstable, first resulting in multicellular secondary flow patterns, and then as the Rayleigh number is further increased the flow becomes chaotic. A high level summary of the expected flow behavior for Cartesian geometry is shown in Figure 1.

The focus in most experimental and computational work is on small aspect ratio cavities ($A = 1 - 5$) including de Vahl Davis [6]. For small aspect ratios the flow characteristics are not multi-cellular and are time invariant.

2.1 Experimental Studies

Several experimental studies have been performed on natural convection in a tall cavity. Table 1 summarizes the natural convection experiments performed. The experimental literature is more extensive for small aspect ratios ($A < 4$).

Most of the experimental work consisted of flow visualization. Most of the authors estimated the observed critical Rayleigh number and the wavenumber.

2.2 Computational Models

The computational models for this problem are summarized in Table 1. All the computational studies unless otherwise noted used the Boussinesq approximation and none of the models considered radiative heat transfer.

Author	Year	Ra	Pr	A	Description
Experimental					
Elder [7]	1965	$1e3 - 1e5$	Silicon	1-60	Streak photos showed multicellular flow.
Vest and Arpaci [17]	1969	$3.7e5$	0.71, 1000	20-33	Streak photos of the flow. Reported Ra_c.
Computational Models					
Vest and Arpaci [17]	1969	$7e3 - 3e5$	0.71, 1000	20-33	Galerkin method.
Korpela et al [10]	1973	$1e2 - 1e4$	0-50	∞	Reported Ra_c.
Bergholz [2]	1978	$1.6e3 - 3e4$	0.73-1000	∞	Galerkin method.
Lee and Korpela [11]	1983	$3e4 - 2e5$	0-1000	15-40	Reported Nu and streamfunctions.
Chenoweth and Paolucci [4]	1986	$1e5 - 1e6$	0.71	1-10	Compare ideal gas and Boussinesq.
Chait and Korpela [3]	1989	$5e2 - 1.5e4$	0.71, 1000	∞	Pseudo spectral method. Reported Ra_c
Le Quere [14]	1990	$7e3 - 4e4$	0.71	16	Explored return to uni-cellular pattern.
Liakopoulos et al. [12]	1990		0.71	10-25	Included flux wall conditions.
Facas [8]	1992	$9e3 - 6e4$	0.71	15	Considered inclined cavities (75^o).
Suslov and Paolucci [16]	1995	$6e3 - 1e4$	0.71	∞	Non-Boussinesq impact on stability and considered Ra_c with ΔT.
Xin and Le Quere [18]	2002	$3e5 - 5e5$	0.71	8	Benchmark study reported Ra_c.
Christon et al. [5]	2002	$1e5$	0.71	8	Comparison study of methods, grids, etc.
Hayden et al. [15]	2003	$7e3 - 3e5$	0.71	33	Commercial code FIDAP.
Present work	2009	$1e4 - 6e5$	0.71	8-33	Commercial code COMSOL.

Table 1: Summary of experimental and computational natural convection studies in a tall cavity.

The computational literature also demonstrates that for low Prandtl number flows the primary instability is a *thermal-shear instability* which obtains kinetic energy primarily from shear production in the flow. Larger Prandtl number flows experience a *thermal-buoyant instability* which obtains energy from the buoyant force.

One of the most interesting papers for the rectangular geometry is the work of Christon et al. [5] which is a compilation of solutions submitted by many participants with a variety of solution methods. The authors found that no specific method (finite element, finite volume, and finite difference) provided superior results. The authors also note that the amplitude of the periodic temperature oscillations can vary by an order of magnitude depending on the specifics of the spatial discretization, grid resolution, governing equations, and solver parameters. Other parameters such as the time averaged velocity were calculated more precisely by the participants. Most importantly, the critical Rayleigh number and the predicted Hopf bifurcation were computed accurately by all methods.

Some authors ([13] and [9]) predict an oscillatory time-dependent instability for tall cavities. Lee and Korpela and Liakopoulos [12] predict that a stationary instability precedes the onset of oscillatory convection for high aspect ratios. Suslov and Paolucci indicate this observation is simply a product of temperature invariant air properties [16]. They also observe that two modes of instability are possible depending on the magnitude

of the temperature difference between the hot and cold wall.

In a similar work Chenoweth and Paolucci [4] observed that as the temperature difference in the cavity increases, a lower critical Rayleigh number is found. They confirmed that the nature of the instability changes with increasing temperature difference.

3 Solution Method

3.1 Governing Equations

The buoyancy driven flow is modeled as a coupled system with fluid motion (Navier Stokes), convection and conduction heat transfer. The governing equations are given in Equations 5-8.

The boundary conditions for the system are specified as adiabatic on the upper and lower cavity boundaries. The right (hot) and left (cold) walls are constrained as constant temperatures as shown in Figure 1.

The weakly compressible Navier Stokes equation for this system is given in simplified form.

$$\rho\frac{\partial u}{\partial t} + \rho(u \cdot \bigtriangledown)u = \bigtriangledown \cdot (-pI + \eta(\bigtriangledown u + \bigtriangledown u^T)) - (2\eta/3 \bigtriangledown \cdot u)I + F \quad (5)$$

$$\bigtriangledown \cdot u = 0 \quad (6)$$

$$\bigtriangledown \cdot (c \cdot \psi) = 0 \quad (7)$$

In this form u represents the velocity vector of the fluid, ρ is the fluid density, η is the dynamic viscosity of the fluid, and F is the force applied to the fluid. Where c is the diffusion coefficient and ψ is the streamfunction. For the models discussed in this section the fluid force is specified in the y-direction for buoyancy driven flow as $F_y = -\rho g$.

The heat transfer convection is governed by Equation 8.

$$\rho c_p \frac{\partial T}{\partial t} + \bigtriangledown \cdot (-k \bigtriangledown T) = -\rho c_p u \cdot \bigtriangledown T \quad (8)$$

For this equation k is the thermal conductivity, c_p is the heat capacity at constant pressure, and T is the temperature.

3.2 Air Properties

The density of the fluid for natural convection systems is often represented with the Boussinesq approximation. The Boussinesq approximation is used for computational problems of this type to simplify the formation of the coupled Navier-stokes equations. The approximation assumes that density variations are small in the fluid except in evaluating the buoyancy force (gravity multiplied by density). In general, the Boussinesq approximation is only valid when the temperature differences in the system are small (less than 28^oC).

For the system considered in this work the Boussinesq approximation is valid, however some authors did observe different results when the air was treated as an ideal gas ([4] and [16]). The experimental results compared in this work involved larger temperature differences. For this reason the Boussinesq approximation was not used and the air was treated as an ideal gas.

Other fluid properties (k, c_p, μ) were all temperature dependent and were defined by using the polynomial fit of Reeve [15].

3.3 Spatial Discretization

For this analysis a grid resolution study was conducted for the $A = 15$ geometry. In the refinement study the density of the mesh was increased and the magnitude and formation of the temperature oscillations was recorded. The mesh was optimized when the formation of the oscillations occurred with the same magnitude and roughly the same iteration time as the most refined mesh. The final mesh was 576 triangular quadratic Lagrangian elements with 5513 degrees of freedom.

4 Numerical Diffusion in COMSOL Multiphysics

Initially a small study was conducted to explore each of the numerical diffusion parameters discussed in this work. In the study a baseline value for each numerical diffusion parameter was taken to be the COMSOL defaults for weakly compressible Navier-Stokes. Each diffusion parameter was then adjusted and a qualitative observation about the effect of altering the parameters on the temperature oscillations in the system was made. It was

found that to most achieve results most closely matching the experimental data required reducing slightly the anisotropic and crosswind diffusion.

The numerical diffusion parameters in COMSOL Multiphysics are outlined in the COMSOL documentation [1], however a short overview of each type is included here along with the results of modifying the values.

- **Isotropic Diffusion.** In COMSOL, isotropic diffusion is equivalent to adding a term to the physical diffusion coefficient. The new term is a tuning parameter (δ_{id}) with recommend values less than 0.5. The effect of isotropic diffusion is to dampen oscillations and impede propagation of oscillations [1]. When isotropic diffusion was introduced in this study it dampened the oscillations or halted them altogether as expected.

- **Anisotropic Diffusion.** Anisotropic diffusion is similar to isotropic diffusion method but occurs only in the direction of the streamline. Like isotropic diffusion, anisotropic diffusion modifies the equation with a new term. The COMSOL documentation suggests values for anisotropic diffusion (δ_{sd}) should be less than 0.5 [1]. In the parametric study conducted for this work the default values of $\delta_{sd} = 0.25$ resulted in values close to the baseline solution. Increasing the anisotropic diffusion reduced the amplitude of the oscillations and had a slight increase of period. Decreasing the anisotropic diffusion increased the amplitude of the oscillations and slightly reduced the period.

- **Streamline upwind Petrov-Galerkin (SUGP).** Streamline diffusion introduces artificial diffusion in the streamline direction. The Streamline upwind Petrov-Galerkin (SUGP) does not perturb the original transport equation. It is closely related to upwinding schemes in finite difference and finite volume methods. SUPG can be shown to add a smaller amount of stability than anisotropic diffusion but yields a higher accuracy than anisotropic diffusion. SUPG is less stabilizing than GLS but is also computationally less expensive. SUPG has the largest effect near the boundary layers [1]. Because SUGP and GLS are closely related the SUGP option was not examined in detail in the baseline study.

- **Galerkin least-squares (GLS).** Galerkin least-squares (GLS) is a more advanced version of SUPG and is of the same order of accuracy. In COMSOL, GLS is the default streamline diffusion mechanism and is part of the baseline solution. In the baseline study GLS was found to be a more robust solution method. In some cases the SUPG failed to converge at all without crosswind diffusion enabled. For this reason GLS was the streamline diffusion method of choice for this work.

- **Crosswind Diffusion.** Crosswind diffusion introduces artificial diffusion in the orthogonal direction to the streamlines. Crosswind diffusion is most useful when undershoots and overshoots can occur in the numerical solutions. Crosswind diffusion methods do not alter the equation but are non-linear [1]. The effect of adjusting the crosswind diffusion coefficient (c_k) in COMSOL for the baseline study was significant. Increasing c_k to 0.2 reduces the oscillations significantly. Decreasing c_k from the baseline smooths the oscillations but does not change the amplitude. A small increase in the period of the oscillations occurs. Removing crosswind diffusion caused the solution to require a much longer time to stabilize and also reduced the period of oscillations.

5 Results

5.1 Numerical Diffusion

Based on the results of the study of the effects of modifying the diffusion coefficients, the subsequent work focused on adjustments to the crosswind diffusion parameter (c_k) and the anisotropic diffusion parameter (δ_{sd}). This analysis was performed for a cavity with $A = 15$. The results are shown in Figure 2-3.

For the anisotropic diffusion Figure 2 (a-c) shows the changes in the streamfunction as the tuning parameter δ_{sd} was changed. In this

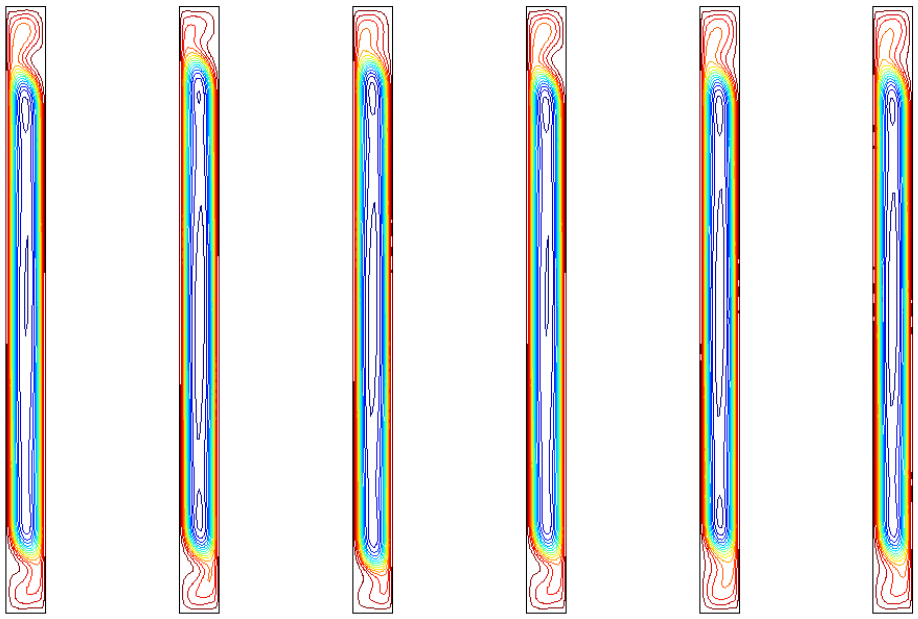

(a) $\delta_{sd} = 0.05$ (b) $\delta_{sd} = 0.15$ (c) $\delta_{sd} = 0.25$ (d) $c_k = 0.01$ (e) $c_k = 0.05$ (f) $c_k = 0.1$

Fig. 2: (a-c) Effect of variation of anisotropic diffusion for $Ra = 1.4e5$, $A = 15$ and $c_k = 0.01$ on the streamfunction at $t = 100$. (d-f) Effect of variation of crosswind diffusion for $Ra = 1.4e5$, $A = 15$ and $\delta_{sd} = 0.05$ on the streamfunction at $t = 100$.

case the structure of the main cell is best defined for the lower values of δ_{sd}. Figure 3 documents the temperature oscillations that occur near the intersection of the cells in the upper half.

For the crosswind diffusion Figure 2 (d-f) shows the changes in the streamfunction as the c_k parameter was adjusted. In this case only slight changes in the streamfunction are visible, primarily near the upper and lower cells. As shown in Figure 3 as c_k is increased oscillations in the cells are halted completely. Over the entire range of Ra examined the higher c_k values prevented the transition to oscillatory convection.

Based on this analysis a low value of crosswind diffusion ($c_k = 0.01$) and a moderate value of anisotropic diffusion ($\delta_{sd} = 0.15$) were chosen for the analysis of larger aspect ratios.

5.2 Small Aspect Ratio (A=8)

Analysis of a small aspect ratio cavity was performed because the benchmark of Xin [18] was very complete. Using the numerical diffusion properties found for $A = 15$ did not give good results for this aspect ratio, and no critical Rayleigh number could be determined. The solution remained time invariant throughout the range of Ra considered. The streamfunction and temperature contours for this aspect ratio appear to be consistent with prior benchmark studies.

The numerical diffusion parameters that give appropriate results for higher aspect ratios ($A > 15$) may not be appropriate for this aspect ratio. It is also possible based on the summary map provided by Chenoweth and Paolucci (Figure 1) that the critical Rayleigh number is affected by the temperature differences examined in this work. Small differences in computational techniques may also be impacting this aspect ratio.

5.3 High Aspect Ratios ($A > 15$)

In all the simulations for the higher aspect ratios the streamfunctions and temperature contours are consistent with those reported in the literature. The streamfunctions are shown in

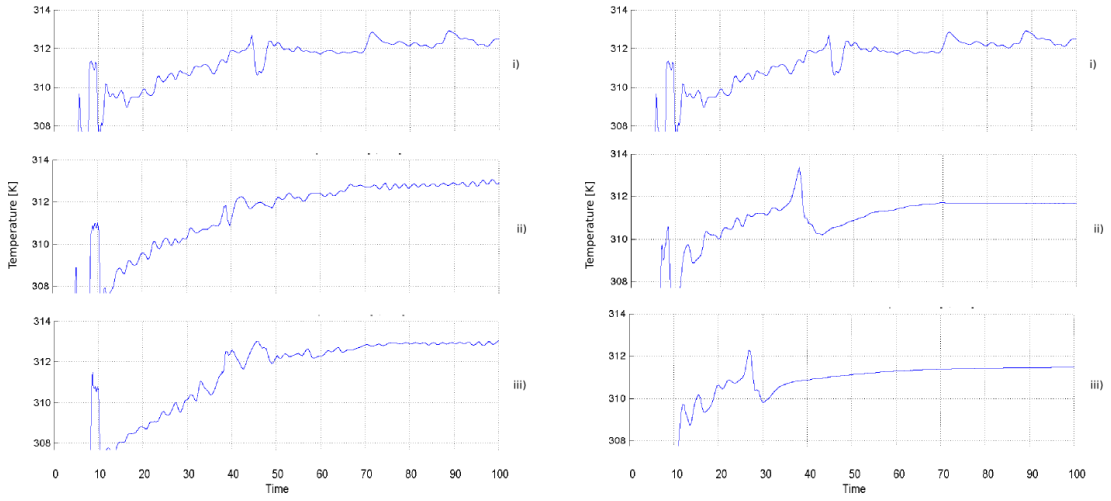

(a) (b)

Fig. 3: Effect of variation of diffusion for $Ra = 2.5e5$, $A = 15$ on the air temperature located at 2/3 of the full cavity height (upper half). a) Diffusion where $c_k = 0.01$. i) $\delta_{sd} = 0.05$ ii) $\delta_{sd} = 0.15$ iii) $\delta_{sd} = 0.25$. b) Diffusion where $\delta_{sd} = 0.15$. i) $c_k = 0.01$ ii) $c_k = 0.05$ iii) $c_k = 0.1$.

Figure 4 and the temperature contours are shown in Figure 5.

Most authors observe a *cat-eye* pattern in flow for high aspect ratios ($A > 12$) that then transitions to a traveling wave instability. In this work, the cat-eye pattern occurred as expected and became traveling waves for $A = 33$.

Analysis of the cavity for $A = 15$ over the range of Rayleigh numbers shows that Ra_c is near 1e5. This is very consistent with the findings of other numerical work [12]. A qualitative comparison of streamfunctions also aligns well with the results of Chenoweth [4] and Liakopoulos [12].

For $A = 20$ the literature reports Ra_c in the range of 1e4 for the onset of multi-cellular motion. A stability transition in this regime was not calculated but the secondary motion transition was found at $Ra = 3.2e4$ which is in good agreement with the stability map of Chenoweth [4]. None of the comparison work for $A = 20$ was based on experimental values for air (Vest and Arpaci report $A = 20$ results for oil), and other authors including Liakopoulos did not have clear computational results for Ra_c at this aspect ratio.

Author	$Ra_{critical}$	Wave Number
$A = 8$		
Xin and Le Quere [18]	3.1e5	1.7
Present work	-	-
$A = 15$		
Liakopoulos et al. [12]	1.4e5	-
Present work	1.4e5	2.62
$A = 20$		
Lee and Korpela [11]	1.1e4	2.82
Liakopoulos et al. [12]	7.1e3	-
Vest and Arpaci [17]	3.7e5	3.5
Present work	3.2e4	-
$A = 33$		
Reeve [15]	6.7e3	2.77
Vest and Arpaci [17]	6.2e3	2.74
Present work	5.8e3	2.49

Table 2: Summary of Cartesian numerical convection studies.

For $A = 33$ the critical Rayleigh number was determined to be $5.8e3$ for the transition

to multi-cellular flow, slightly below the experimental value determined by Vest and Arpaci. This value is also consistent with other numerical studies. As the Rayleigh number was increased the period of the waves in the simulation decreased. The critical wavenumber for this computational work agrees well with the experimental work of Vest and Arpaci [17] but improvements may be possible.

Table 2 provides a summary of all the critical Rayleigh numbers determined by prior authors and the present work.

6 Conclusion

The comparison with experimental work indicates that by tuning the numerical diffusion it is possible to match the values the critical Rayleigh numbers and wave lengths for high aspect ratio cavities with natural convection. The critical Rayleigh numbers agree well with the experimental results of Vest and Arpaci [17] for $A = 33$. A further analysis of the effect of this numerical diffusion may be required to understand if the low aspect ratio case (A=8) can give better agreement.

In general, COMSOL was found to give appropriate qualitative stream functions and temperature contours for all aspect ratios. The critical Rayleigh numbers for the simulations decrease as the aspect ratio is increased which is consistent with prior work in the literature. That the values of δ_{sd} and c_k that were found to be optimum for A=15 were also appropriate for the higher aspect ratios provides additional assurance to users of COMSOL Multiphysics.

References

[1] *Comsol user's guide.*

[2] R.F. Bergholz, *Instability of steady natural convection in a vertical fluid layer*, Journal of Fluid Mechanics (1978).

[3] A. Chait and S.A. Korpela, *The secondary flow and its stability for natural convection in a tall vertical enclosure*, Journal of Fluid Mechanics (1989).

[4] D.R. Chenoweth and S. Paolucci, *Natural convection in an enclosed vertical air layer with large horizontal temperature differences*, Journal of Fluid Mechanics (1996).

[5] M.A. Christon, P.M. Gresho, and S.B. Sutton, *Computational predictability of time-dependent natural convection flows in enclosures (including a benchmark solution)*, International Journal for Numerical Methods in Fluids (2002).

[6] G. de Vahl Davis, *Natural convection of air in a square cavity: A bench mark numerical solution*, International Journal for Numerical Methods in Fluids (1983).

[7] J. Elder, *Laminar free convection in a vertical slot*, Journal of Fluid Mechanics (1965).

[8] G. Facas, *On the convective instability in long inclined cavities*, ASME Stability of Convective Flows (1992).

[9] P. Haldenwang and G. Labrosse, *2-d and 3-d spectral chebysheve solutions for free convection at high rayleigh number*, Sixth International Symposium on Finite Element Methods in Flow Problems (1986).

[10] S.A. Korpela, D. Gozum, and C.B. Baxi, *On the stability of the conduction regime of natural convection in a vertical slot*, International Journal Heat and Mass Transfer (1973).

[11] Y. Lee and S. A. Korpela, *Multicellular natural convection in a vertical slot*, Journal of Fluid Mechanics (1983).

[12] A. Liakopoulos, P.A. Blythe, and P.G. Simpkins, *Convective flows in tall cavities*, Simulation and Numerical Methods in Heat Transfer (1990).

[13] S. Paolucci and D.R. Chenoweth, *Transition to chaos in a differentially heated vertical cavity*, Journal of Fluid Mechanics (1989).

[14] P. Le Quere, *A note on multiple and unsteady solutions in two-dimensional convection in a tall cavity*, Journal of Heat Transfer (1990).

[15] Hayden Reeve, *Effect of natural convection heat transfer during polymer optical fiber drawing*, Ph.D. thesis, University of Washington, 2003.

[16] S.A. Suslov and S. Paolucci, *Stability of natural convection flow in a tall vertical enclosure under non-boussinesq conditions*, International Journal of Heat and Mass Transfer (1995).

[17] C.H. Vest and V.S. Arpaci, *Stability of natural convection in a vertical slot*, International Journal of Fluid Mechanics (1969).

[18] S. Xin and P. Le Quere, *An extended chebyshev pseudo-spectral benchmark for the 8:1 differentially heated cavity*, International Journal for Numerical Methods in Fluids (2002).

Acknowledgments

These results were obtained as part of the research supported by the National Science Foundation through Grant 0626533.

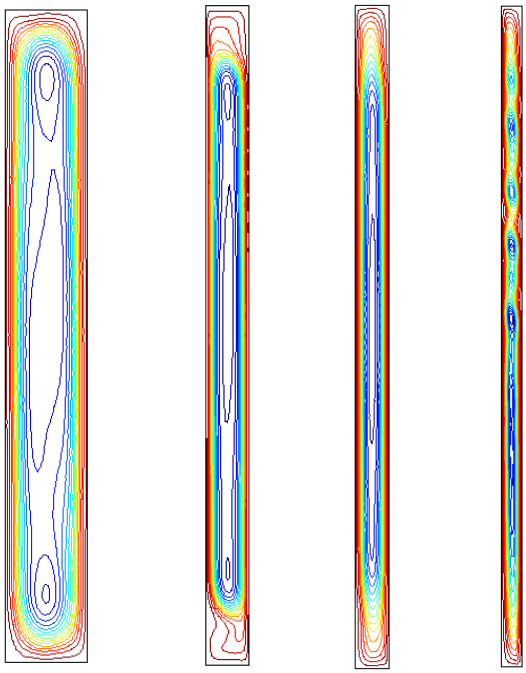

(a) A=8 (b) A=15 (c) A=20 (d) A=33

Fig. 4: Streamfunction for $Ra = 1.6e5$ at $t = 100$.

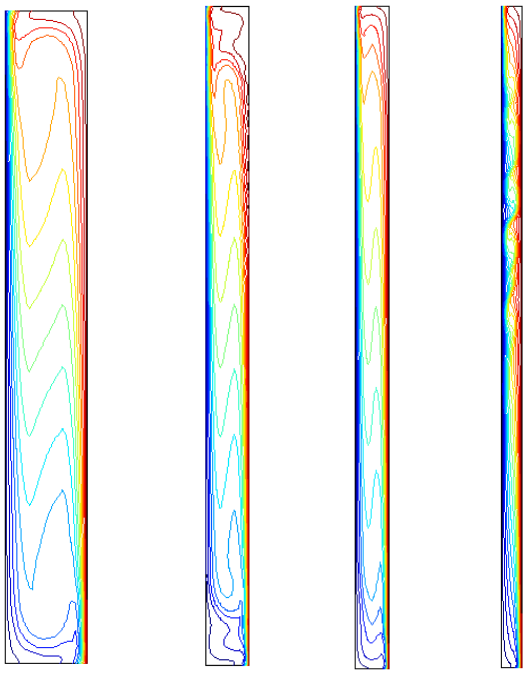

(a) A=8 (b) A=15 (c) A=20 (d) A=33

Fig. 5: Temperature contours for $Ra = 1.6e5$ at $t = 100$.